

A Novel Circularly polarized dielectric resonator antenna with Branch-Line Coupler and Log-Periodic Balun

Z. Rahimian, S. Nikmehr, and A. Pourziad

Department of Electrical and Computer Engineering, University of Tabriz, Tabriz, Iran
Rahimian@tabrizu.ac.ir, Nikmehr@tabrizu.ac.ir, and ali_pourziad@tabrizu.ac.ir

Corresponding author: Rahimian@tabrizu.ac.ir

Abstract-A new shaped circularly polarized dielectric resonator antenna (CP DRA) is studied with branch-line coupler and log-periodic balun for the GPS application. Since the coupler and balun are located under the DRA, it does not increase the footprint of the antenna, as a result the system is very compact. Two configurations are considered in this paper. In the first configuration, an external 50Ω load is used for the matching port of the branch-line coupler. For the second one, a three-resonator log-periodic balun is used instead of branch-line coupler, thus, no lumped elements are required in this configuration. Moreover, two modes $HE_{11\delta}$ of the cylindrical DRA are utilized to design the wide band circular polarization. The reflection coefficient, axial ratio, antenna gain, and radiation pattern are studied for each configuration. These first and the second configurations offer an impedance bandwidth ($S_{11} < -10\text{dB}$) of 59.7% and 58.8%, and axial ratio bandwidth ($AR < 3\text{dB}$) of 58% and 55%, respectively.

Index Terms-Circular polarization, dielectric resonator antenna, coupler, balun.

I. INTRODUCTION

Due to a number of attractive features such as its small size, low loss, wide bandwidth, and ease of excitation, the dielectric resonator antenna (DRA) has been studied extensively in the past two decades [1]-[3]. Various antenna geometries, excitation schemes, and bandwidth enhancement techniques have been developed for the designs of DRA. A considerable portion of these studies have been focused on the dielectric resonator antenna (DRA) with circular polarization. Circularly polarized antennas are widely used in various communication systems including satellite positioning and broadcast, portable communications, and radar systems [4]. It is due to several advantages of circularly polarized antennas, as compared with linearly polarized antennas, such as more flexibility to the orientation between the transmitter and receiver antennas and less sensitivity to propagation effects. Several techniques have been proposed to generate CP using DRAs. These techniques can be

classified into three categories: 1. using a single port, 2. using a single port to excite two modes, and 3. using multiple ports to excite two modes. The first method makes use of a single port and change in the geometry conditions of DR to excite degenerate modes, in order to generate CP fields. For example specially shaped DRAs have been investigated in [5], [6]. These designs make use of slots on the side walls of DRAs to excite degenerate modes, in order to generate CP fields with 3dB AR bandwidth of 8.2%. The second method applies a single port and ordinary DR to excite two modes which are geometrically orthogonal and quasi-degenerate. The quasi-degeneracy of the modes provides the phase quadrature between the modes. For example the bowtie cross-slot coupled cylindrical DRA with 3dB AR bandwidth of 17.24% has been reported in [7]. The rectangular DRA with a square spiral microstrip feed line, with 3dB AR bandwidth of 15.5%, has been reported in [8]. A CP quadruple strip fed cylindrical DRA utilizing a pair of 90° hybrid couplers and providing an axial ratio bandwidth of 25.9% has been investigated in [9]. Reference [10] describes design of a dual wide-band cylindrical DRAs to obtain CP fields with the quadrature strip-fed method. They reported a measured 3dB AR bandwidth of 24.7%. A CP rectangular DRA with dual underlaid hybrid couplers has been investigated for the first time, with 3dB AR bandwidth of 27.7% in [11]. The design of a broadband dual-feed type CP rectangular DRA has been presented in [12]. Its feed network consists of a 3dB Wilkinson power divider and a wideband 90° phase shifter. In this case 3dB AR bandwidth obtains 41.7%. The third method employs multiple ports in order to excite two modes which are geometrically orthogonal. The multiple feeds are used to create the phase quadrature between the modes. For example a rectangular DRA fed by two vertical strips which are quadrature in phase was studied in [13]. In reference [14] a cylindrical DRA fed by four sequentially rotated slots was investigated and good AR bandwidth for covering satellite navigation systems was obtained.

In this paper, the proposed antenna structure includes cylindrical and conical DR that is integrated with each other. The DR lies on top of a branch-line coupler (first antenna). The branch-line coupler is used to generate two quadrature signals, which are fed to two vertical excitation strips stuck on the side wall of the cylindrical DRA. Two modes $HEM_{11\delta}$ of the cylindrical DRA are utilized to design the wide band circular polarization. The above proposed configuration uses an external 50Ω load in designing the branch-line coupler, which is a very conventional approach. Apart from configuration, this paper also investigates a second configuration (second antenna) that does not require any lumped elements. The new design makes use of a three-resonator log-periodic balun instead of branch-line coupler. This is the main advantages regarding to the first antenna. It is worth mentioning despite simplifying the second antenna the results for both first and second antenna remain approximately unchanged. With this approach, a wide AR bandwidth of 55% can be obtained. It can be seen that this bandwidth is very close to the first configuration. In this paper the main differences of the proposed antenna compared to the previous paper were using a few simple techniques simultaneously to improve results of antenna. These techniques are as follow: (1) Using three-

resonator log-periodic balun instead of branch-line coupler, thus, no lumped elements are required in this configuration. (2) Placing the coupler (balun) under DR with 45° rotation instead of horizontal or vertical situation, this insertion is the best choice because of no extra space is needed for the coupler (balun), making the system very compact. Also with this compact configuration, loss of the feed network and, hence, reduction in the antenna gain, can be minimized. (3) Using cylindrical and conical DR that is integrated with each other, a new shaped dielectric resonator antenna is obtained. In addition, the idea of improving gain by DR cone is introduced in this paper. The proposed antenna structure can operate all GPS bands (L1\L2\L3\L4\L5) and has high gain. Also, this antenna element has a low axial ratio over wide frequency band and a wide bandwidth which is more than what is needed for GPS applications. It is well suited to practical applications for satellite.

II. CONFIGURATIONS OF THE CIRCULARLY POLARIZED DRAS

The CP DRAs design using branch-line coupler and log-periodic balun is given in this section. Fig. 1 show the first configuration DRA. In addition, Fig. 2 shows the second configuration, which is designed by log-periodic balun. The proposed antenna structure includes cylindrical and conical DR that is integrated with each other. The cylindrical part of DRA has a radius $R_1=30$ mm, height $H=20$ mm, and dielectric constant $\epsilon_r=9.8$. According to reference [1], in the dielectric resonator antennas with high dielectric constants have lateral dimensions that are comparable to patch antennas with low dielectric constants. However, even the low-profile dielectric resonator antennas are usually taller than the patch counterparts. Also, despite the high dielectric constant, the DR antennas have wider bandwidths, both for the axial ratio and the impedance bandwidth. The cone of the antenna includes a conical dielectric $\epsilon_r=9.8$, height $H_c=30$ mm, and radius $R_1=30$ mm, and $R_2=0$ mm, respectively. Also, our extensive parametrically simulation results about different dimension of the antenna, lead to optimized dimensions for the center frequency.

A. The First Antenna Geometry and Design

The first DRA was designed to resonate in GPS band. The DRA is mounted on the branch-line coupler. Two modes $HEM_{11\delta}$ of the cylindrical DRA are utilized to design the wide band circular polarization.

The coupler is used to generate two quadrature signals, which feed two vertical exciting strips on the side walls of the DRA to generate CP fields [15]. As can be seen from the figure, two flat metallic excitation strips which are cut from a copper tape are stuck on the DR to quadraturely feed the DRA. They have width $W_{strip}=3$ mm, and vertical length $H_{strip}=15$ mm. The results revealed that the conformal excitation strips can efficiently couple electromagnetic energy to the DRA.

The branch-line coupler is designed on a low-cost FR4 substrate with dielectric constant $\epsilon_{sub}=4.4$, thickness $S=0.8$ mm, and size of $75\text{ mm}\times 75\text{ mm}$.

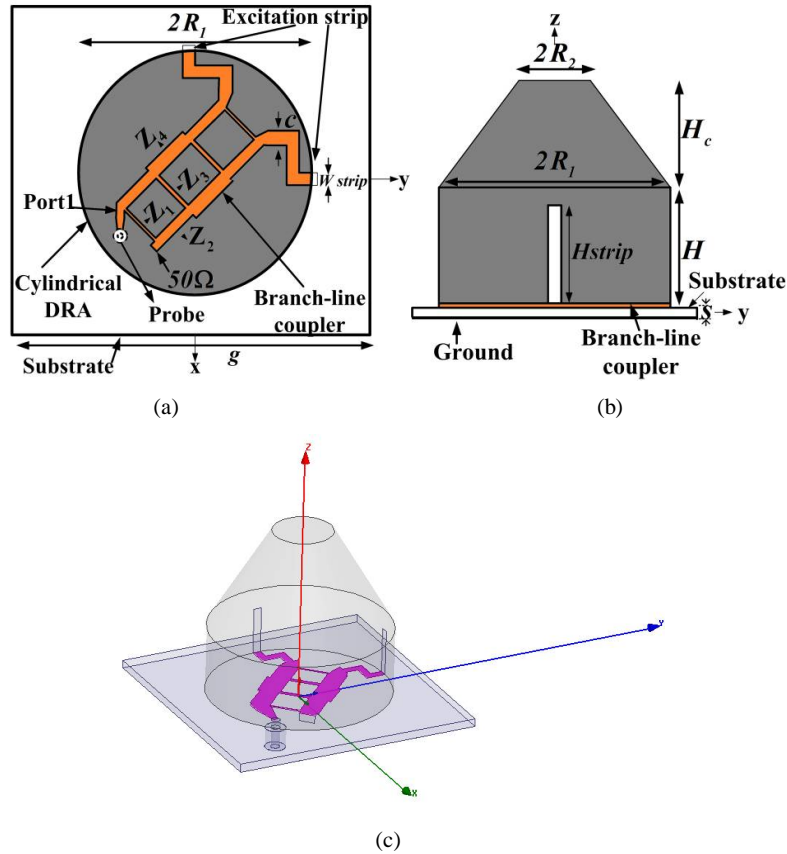


Fig. 1. First antenna with an underlaid branch line coupler. An external 50Ω load is used for the matching port of the coupler.

(a) Top view. (b) Front view. (c) 3D view

The configuration of the coupler is presented in Fig. 1(a). It involves four vertical and six horizontal $\lambda_g/4$ lines [15]. The optimized values of the characteristic impedances are determined as: $Z_1=175.2\Omega$, $Z_2=95.1\Omega$, $Z_3=118.4\Omega$, $Z_4=62.9\Omega$, and $Z_0=50\Omega$. Also the isolated port of the coupler is terminated in a 50Ω external load. A coaxial probe is used to deliver the power to the input port of the coupler through a tapered stub with length of $\lambda_g/4$. The tapered stub makes the waves traverse a longer path to arrive at port 1.

B. The Second Antenna Geometry and Design

The top view of the second configuration is shown in Fig. 2. A three-resonator log-periodic balun operating in the range of 1-2 GHz is used instead of branch-line coupler in the second antenna. This configuration does not need any lumped elements for the matching port.

This balun consists of quarter-wave resonators and generate two quadrature signals, which are fed to two vertical excitation strips stuck on the side wall of the cylindrical DRA. In a balun having odd number of cells, the length of the resonator in the central cell is made equal to $\lambda_{gc}/4$, where λ_{gc} is the

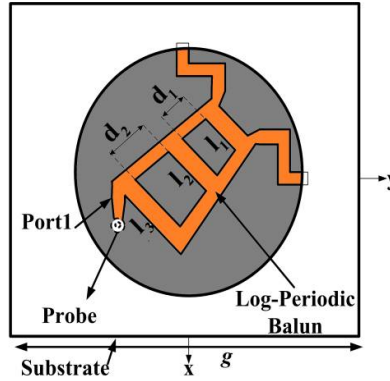


Fig. 2. Top view of the second antenna. A log-periodic balun is used. No lumped elements are required in this configuration.

guide wavelength in microstrip at the band center frequency. The substrate is low-cost FR4 having a dielectric constant of 4.4 and thickness of 0.8 mm.

The transmission lines to be used are microstrip lines, having $Z_0 = 50 \Omega$. At the band center frequency (1.5GHz), λ_{gc} is 107.4 mm. The geometric ratio τ was chosen to be $\tau = 0.95$. Using the design equation (1), the lengths of the resonators and the distances between them were found [16]. A coaxial probe is used to deliver the power to the input port of the balun through a tapered stub. The same parameter values as in the case of the first antenna are used for the second antenna. Each strip for the second antenna has a length of $H_{strip} = 18$ mm and a width of $W_{strip} = 3$ mm.

$$\begin{aligned}
 L_1 &= \tau^2 \lambda_{gc} / 4 & d_1 &= \frac{(L_1 + L_2)}{2} \\
 L_2 &= \lambda_{gc} / 4 & d_2 &= \frac{(L_2 + L_3)}{2} \\
 L_3 &= L_2 / \tau & &
 \end{aligned} \tag{1}$$

III. SIMULATION RESULTS AND DISCUSSIONS

In this part, the performance of the proposed antenna is discussed according to results of simulation. For each configuration, Ansoft HFSS was used to study the reflection coefficient, axial ratio, radiation pattern, and antenna gain. Likewise, the simulation results were confirmed using CST Microwave Studio which is based on finite integral technique.

A. The First antenna Results and Discussion

With regard to the first configuration, phase difference between two ports of coupler in both HFSS and CST Microwave shows in Fig. 3. The coupler can excite two orthogonal degenerate modes which a 90° phase difference which produce a circularly polarized radiation field. Small phase-variations (less than $\pm 10^\circ$) are realized across the designed frequency range.

A plot of the reflection coefficient for the first CP DRA versus frequency is provided in Fig.4(a). This figure shows that our proposed antenna can fully cover the frequency band of 1.08-2 GHz (GPS) and simulated -10dB impedance bandwidth is 59.7% Fig.4(b) shows the simulated AR in the

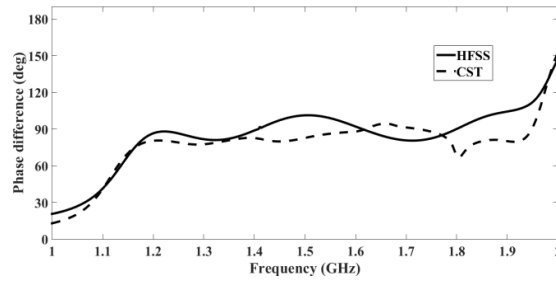
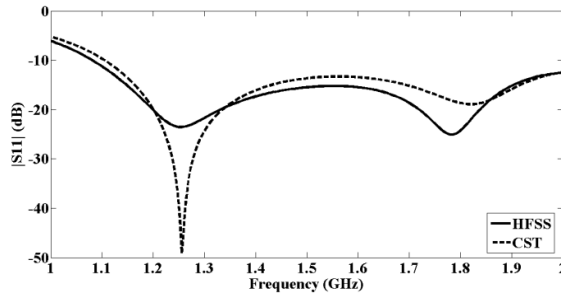
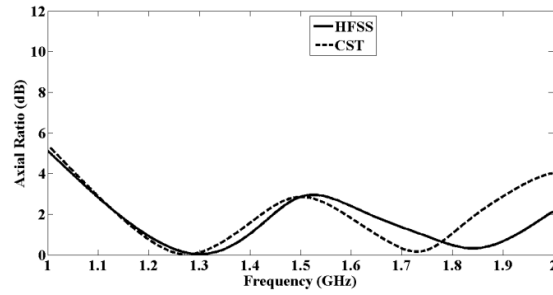


Fig. 3. Phase difference between two ports of coupler.



(a)



(b)

Fig. 4. Simulated results of the first antenna. (a) Reflection coefficient magnitude (S11), (b) Axial ratio.

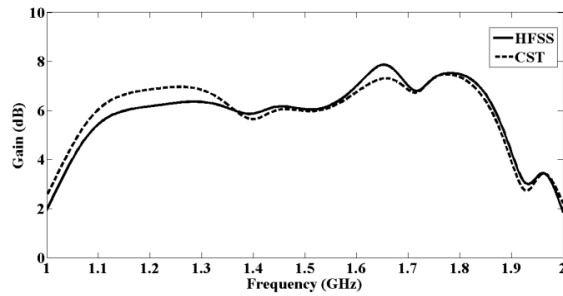


Fig. 5. Simulated gain of the first antenna.

boresight direction ($\theta = 0^\circ$). A wide 3dB AR bandwidth of 58% (1.1-2 GHz) is obtained, which is more than what is needed for GPS applications. Obviously, it can be inferred that there is a good agreement between HFSS and CST.

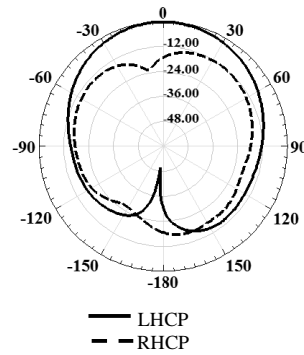


Fig. 6. Simulated radiation pattern (LHCP and RHCP) of the first antenna. The simulation was done at 1.28GHz in xz-plane.

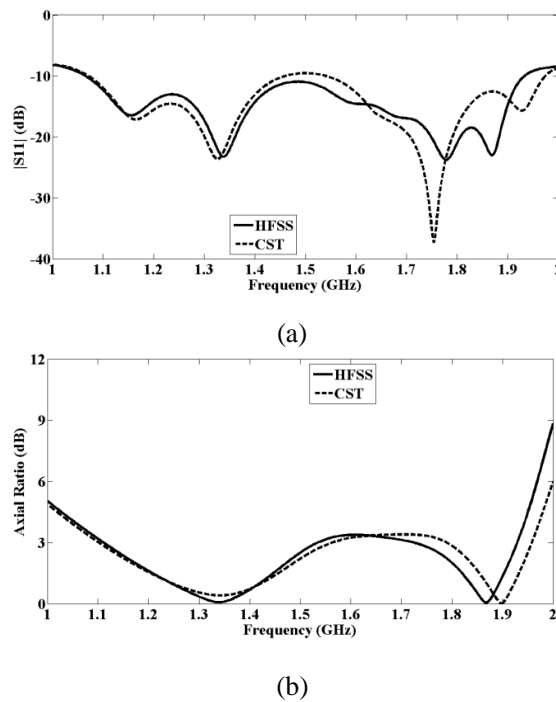


Fig. 7. Simulated results of the second antenna: (a) Reflection coefficient magnitude (S11), (b) Axial ratio.

As it can be seen from Fig. 5, the simulated antenna gain varies between 2dB and 8dB while the simulated peak gain is given by 8 dB at 1.65 GHz. The agreement between the results of HFSS and CST is quite good. Fig. 6 represents the simulated radiation patterns at 1.28 GHz for xz-plane. With reference to this figure, it can be inferred that the LHCP fields are stronger than RHCPs.

B. The Second Antenna Results and Discussion

With regard to the second configuration (Fig.2), Fig.7(a) shows the simulated reflection coefficient of the second antenna, which represents that, the simulated -10dB impedance bandwidths are 58.8% (1.08–1.98 GHz). The simulated AR in the boresight direction ($\theta = 0^\circ$) is depicted in Fig.

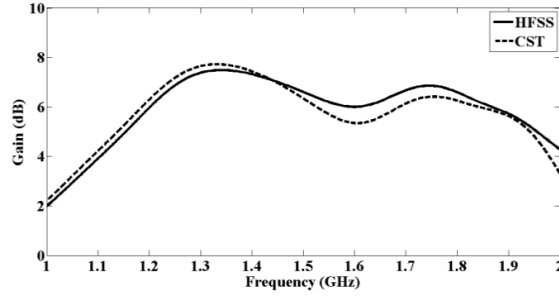


Fig. 8. Simulated gain of the second antenna.

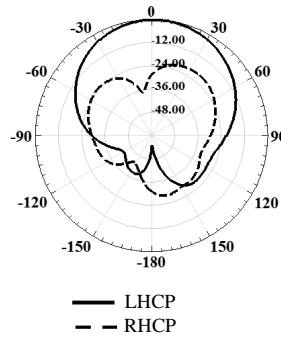


Fig.9. Simulated radiation pattern (LHCP and RHCP) of the second antenna. The simulation was done at 1.35 GHz in xz-plane.

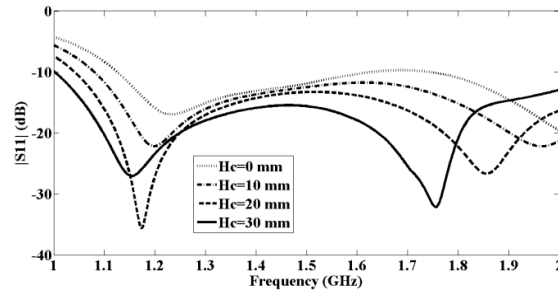
7(b). It can be observed that a wide 3dB AR bandwidth of 55% (1.1–1.93 GHz) is obtained.

Clearly, a good agreement between HFSS and CST has been obtained. It is found that bad impedance matching at around 1.55 GHz can result in a poor AR value. It can be expected that the both impedance and axial ratio bandwidth are as wide as they were for the first configuration. Fig.8 shows the simulated antenna gain. The simulated peak gain is given by 7.8 dB at 1.3 GHz. The agreement between the results of HFSS and CST is reasonably good. Fig.9 shows the simulated radiation pattern at 1.35GHz for xz-plane. Referring to the figure, we realize that the LHCP fields are stronger than the RHCPs.

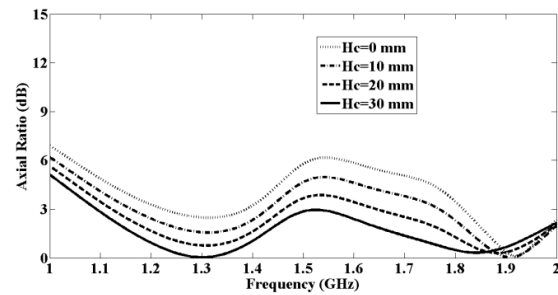
C. Parametric Study

Parametric studies by using HFSS simulator were conducted on an early variant of the first antenna in order to understand how best to tune for wide axial ratio (AR) bandwidth, and impedance matching. This study incorporated two parameters, the heights of the cone (H_c) and Radius of the cone (R_2). These parameters are shown graphically in Fig. 1.

In the design process, the effect of various lengths of the cone (H_c) was investigated which is shown in Fig.10. Through simulation, the researchers found that with $H_c = 30$ mm, a good result can be obtained. H_c was swept from 0mm to 30mm in 10mm steps. As it is shown in Figs.10(a) and 10(b), the Heights of the cone (H_c) have a pronounced effect on both impedance match (S_{11}) and



(a)



(b)

Fig. 10. Effects of different Hc on the first antenna: (a) Reflection coefficient magnitude (S11), (b) Axial ratio

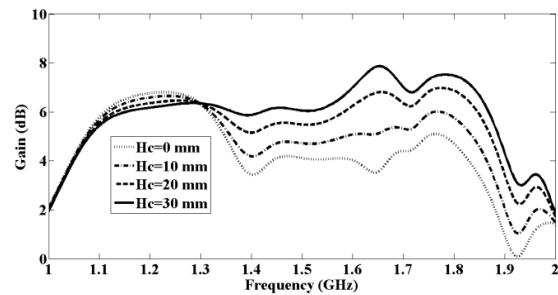


Fig. 11. Simulated gain of antenna with different Hc.

axial ratio versus frequency. An interesting point, here, is that increasing Hc leads to better impedance matching and wider AR bandwidth. As Hc is increased, the impedance match and AR bandwidth moves down in frequency band. Fig. 11 shows the first antenna gain for different Hc. In most parts of the GPS band, the peak gain of antenna increases by increasing the length of the cone. This is due to the fact that by increasing DR cone, antenna gain improves.

The radius (R2) has more importance and effect on the resonance frequency. R2 was swept from 0mm to 30mm in 10mm steps. Figs. 12(a) and 12(b) show the response for R2 in relation to impedance match and AR bandwidths. As R2 is decreased, the resonance becomes more defined and impedance match improves, as a result AR performance increase.

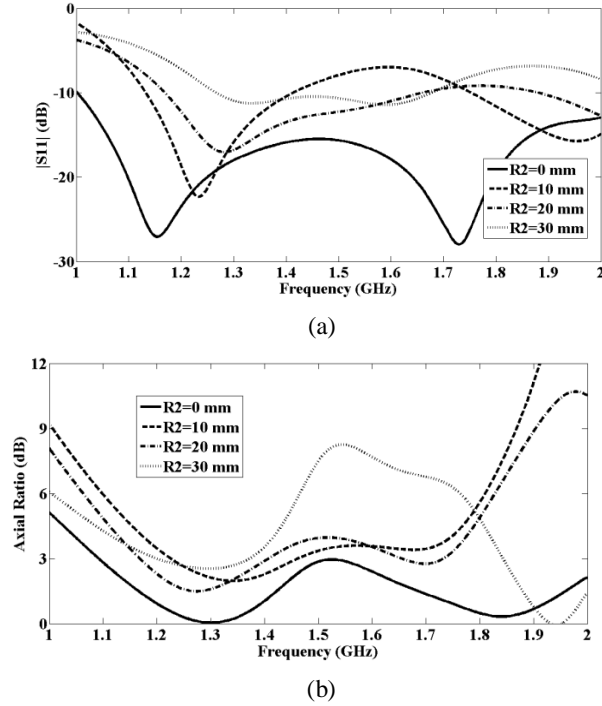


Fig. 12. Effects of different R2 on the first antenna: (a) Reflection coefficient magnitude (S_{11}), (b) Axial ratio

TABLE I. Summary of characteristics of proposed antenna and antennas in references [8, 9]

Reference	-10dB reflection bandwidth(%)	3dB AR Bandwidth(%)	Gain (dB)	Size (mm× mm× mm)
[8]	34.5%	25.9%	4.95	200×200×20
[9]	25.5%	24.7%	6.73	100×100×34.3
First antenna	59.7%	58%	8	75×75×50
Second antenna	58.8%	55%	7.8	75×75×50

Finally, Table I shows a comparison between the proposed antenna and antennas in references [8, 9] in terms of the reflection coefficient, 3dB AR bandwidth, gain, and size. It can be seen that the results for both first and second antenna are close to each other and better than the antennas in references [8, 9].

CONCLUSION

The present paper proposed a new shaped circularly polarized dielectric resonator antenna which is very compact because it does not require any extra space to accommodate the quadrature feed network. Two configurations were considered. The first configuration had an external 50 Ω load for the matching port of the branch-line coupler, whereas the second one made use of log-periodic balun without using any lumped elements to provide the 50 Ω load. It was found that the proposed antenna

structure can operate all GPS bands and has high gain. The idea of improving gain by DR cone is, also, introduced in this study.

REFERENCES

- [1] K. M. Luk and K. W. Leung, "Dielectric Resonator Antennas," *Eds. London, U. K: Research Studies Press*, 2003.
- [2] M. Bemani, S. Nikmehr, and H. Younesiraad, "A Novel Small Triple Band Rectangular Dielectric Resonator Antenna for WLAN and WiMAX Applications," *J. of Electromagn.. Waves and Appl.*, vol. 25, no. 11-12, pp.1688-1698, April 2011
- [3] MohdFadzilAina, UbaidUllahb, and ZainalArifinAhmada, "Bi-polarized Dual-segment Rectangular Dielectric Resonator Antenna," *IETE Journal of Research*, vol. 59, no. 6, pp. 739-744, 2013.
- [4] Yong Mei Pan, Kwok Wa Leung, and Kai Lu, "Omnidirectional linearly and circularly polarized rectangular dielectric resonator antennas," *IEEE Trans Antennas Propag.*, vol. 60, no.2, pp.751-759, Feb. 2012
- [5] Y. M. Pan and K. W. Leung, "Wideband omnidirectional circularly polarized dielectric resonator antenna with parasitic strips," *IEEE Trans Antennas Propag.*, vol. 60,no. 6, pp. 2992-2997, June 2012.
- [6] J. M. Patin and S. K. Sharma, "Single feed aperture-coupled wideband dielectric resonator antenna with circular polarization for Ku-band applications," *International Journal of Antennas & Propag.*, May 2012.
- [7] Lei Zhang, Yong-Chang Jiao, and Zi-Bin Weng, "Wideband circularly polarized dielectric resonator antenna with a square spiral microstrip feedline," *Progress in Electromagnetics Research Letters*, vol. 41, pp.11-20, 2013.
- [8] Kah-Wee Khoo, Yong-XinGuo, and Ling ChuenOng, "Wideband circularly polarized dielectric resonator antenna," *IEEE Trans Antennas Propag.*, vol. 55,no.7,pp.1929-1932, July 2007.
- [9] Xiao Sheng Fang, and Kwok Leung, "Linear-/circular polarization designs of dual-/wide-band cylindrical dielectric resonator antennas," *IEEE Trans Antennas Propag.*, vol. 60,no.6,pp.2662 -2671, June 2012.
- [10] Yongmei Pan, Kwok Wa Leung, and Eng Hock Lim, "Compact wideband circularly polarized rectangular dielectric resonator antenna with dual overlaid hybrid couplers," *Microwave Opt. Technol. Lett.*, vol. 52, no. 12, pp.2789-2791, Dec. 2010.
- [11] Rong-Cang Han, Shun-Shi Zhong, and Jing Liu, "Design of broadband circularly polarized dielectric resonator antenna using improved feed network," *Microwave Opt. Technol. Lett.*, vol.56, no. 9, pp.2191-2195, Sept. 2014.
- [12] Bin Li, Cheng-Xiang Hao, and Xin-Qing Sheng, "A dual-mode quadrature-fed wideband circularly polarized dielectric resonator antenna," *IEEE Antenna Wireless Propag. Lett.*, vol. 8, pp.1036-1038, 2009.
- [13] Gabriel Massie, Mathieu Caillet, Michel Clénet, and Yahia M. M. Antar, "A new wideband circularly polarized hybrid dielectric resonator antenna," *IEEE Antenna Wireless Propag. Lett.*, vol. 9, pp.347 -350, 2010.
- [14] K. W. Leung, W. C. Wong, K. M. Luk, and E. K. N. Yung, "Circular-polarized dielectric resonator antenna excited by dual conformal strips," *Electronics Letters*, vol. 36, no. 6, pp.484-486, March 2000.
- [15] Yuandan Dong, and Tatsuo Itoh, "Planar ultra-wideband antennas in Ku- and K-band for pattern or polarization diversity applications," *IEEE Trans Antennas Propag.*, vol. 60, no. 6, pp.2886 -2895, June 2012.
- [16] Mahmoud Al Basraoui, Prasad N. Shastry, "Wideband planar log-periodic balun," *International Journal of RF and Microwave Computer Aided Engineering*, vol. 11, no. 6, pp.343-353, Nov. 2001.